Lau, C. K. & Bolton, M. D. (2011). *Géotechnique* **61**, No. 8, 627–638 [**doi:** 10.1680/geot.7.00206]

The bearing capacity of footings on granular soils. I: Numerical analysis

C. K. LAU* and M. D. BOLTON†

The method of characteristics has been used to determine the bearing capacity of shallow foundations, in either plane-strain or axisymmetric condition. Most previous solutions for granular soils were based either on a straight (c, ϕ) envelope or simply on a constant angle of shearing, ϕ. For granular soils, $\sec\phi$ usually varies linearly with the logarithm of mean effective stress. A new method of calculation permits ϕ to vary throughout the stress field as an arbitrary (or empirical) function of stress. This method is verified for both plane-strain and axisymmetric conditions by forcing a variation in $\sec\phi$ equivalent to generating a constant-cohesion envelope, for which solutions already exist. The variable-ϕ analysis is used to demonstrate the highly significant effect of stress variation around and beneath a footing. Finally, it is shown that an equivalent constant value ϕ_m can be derived empirically, using the new solutions to identify an equivalent mean effective stress p_m. However, only the variable-ϕ solution can simultaneously capture the bearing capacity and the geometry of the bearing mechanism.

KEYWORDS: bearing capacity; footings/foundations; numerical modelling; plasticity; shear strength; stress analysis

On a utilisé la méthode des caractéristiques pour déterminer la force portante de fondations superficielles, soit en déformation biaxiale, soit dans des conditions axisymétriques. La plupart des solutions précédentes pour sols granulaires étaient basées sur une enveloppe droite (c, ϕ) ou, simplement, sur un angle de cisaillement constant ϕ. Il convient de reconnaître que la sécante ϕ pour sols granulaires varie généralement de façon linéaire en fonction du logarithme de la tension efficace moyenne. Une nouvelle méthode de calcul permet à ϕ de varier dans l'intégralité du champ des contraintes en tant que fonction arbitraire (ou empirique) de la contrainte. Cette nouvelle méthode de calcul est vérifiée aussi bien dans les déformations planes que dans des conditions axisymétriques, en forçant une variation dans la sécante ϕ équivalente à la production d'une enveloppe à cohésion constante, pour laquelle il existe déjà des solutions. L'Analyse variable-ϕ sert à démontrer l'effet extrêmement significatif des variations de contrainte autour d'une semelle, et sous celle-ci. Enfin, on démontre qu'il est possible de dériver de façon empirique une valeur ϕ_m constante équivalente, en utilisant les nouvelles solutions pour identifier une tension efficace moyenne équivalente p_m. Toutefois seule la solution à variable-ϕ est en mesure de capturer simultanément la force portante et la géométrie du mécanisme porteur.

INTRODUCTION

Triaxial test results by De Beer (1965), shown in Fig. 1, have clearly shown that $\sec\phi$ is not a material constant for granular soils, but is extremely sensitive to the mean stress level. For the purpose of this paper, all stresses are effective stresses unless otherwise stated. The vertical stress in the supporting soil ranges from the bearing capacity σ_f directly under the footing to the overburden pressure σ_o on either side (see Fig. 2). The stress can vary by a factor of up to 1000 for high ϕ values in constant-ϕ analysis (Bolton & Lau, 1993). The contact stress distribution under the footing is also highly non-uniform. The stress tends to be highest at the centre and eases off rapidly towards the edge, especially for shallow circular footings. Stress variations therefore cause ϕ_m to vary significantly from point to point.

Constant-ϕ analysis ignores the 7° change in ϕ_{max} as a result of the tenfold change in confining pressure observable in Fig. 1, and typical for a dense sand. Such analysis is therefore incapable of accurately representing the true situation. Ueno *et al.* (1998) reported good agreement with test data for both strip and circular footings in their non-linear finite-element analysis, after incorporating the confining-stress-dependent shear strength. Kumar & Khatri (2008) reported similar results for smooth strip footings.

A new form of analysis that takes the pressure effects on ϕ into account will be investigated below. Essentially, the calculations will use the ϕ value corresponding to the locally prevailing stress level.

Bolton's (1986) work on the strength and dilatancy of sands accounts for the variation in secant angle ϕ rather than attempting to define the Mohr–Coulomb envelope Fig. 3(a). Attempts to fit a straight c–ϕ envelope (Kutter *et al.*, 1988) proved successful when the envelope was fitted over the appropriate stress range. Fig. 3(b) demonstrates, however, that for a stress range of 0–10 MPa that involves crushing

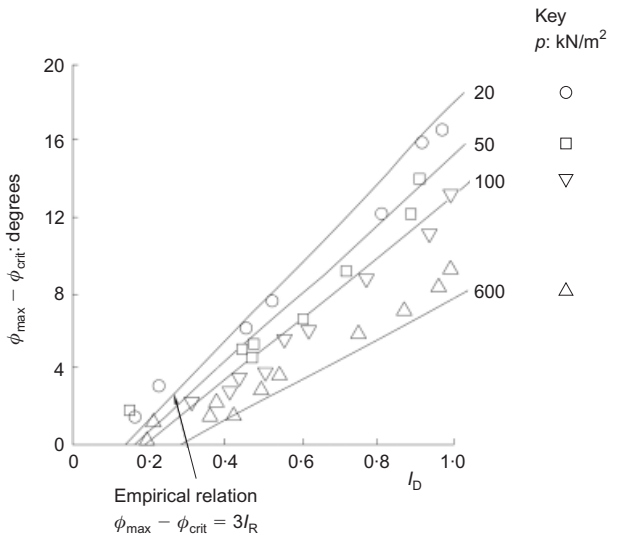

Fig. 1. Triaxial test data for Berlin sand (after De Beer, 1965)

Manuscript received 27 November 2007; revised manuscript accepted 15 October 2010. Published online ahead of print 25 January 2011. Discussion on this paper closes on 1 January 2012, for further details see p. ii.

* Fong On Geotechnics Limited, Hong Kong.
† Engineering Department, University of Cambridge, UK.

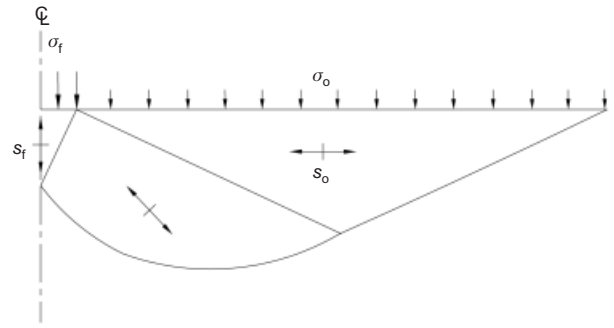

Fig. 2. Principal stress directions beneath a collapsing strip footing on weightless soil

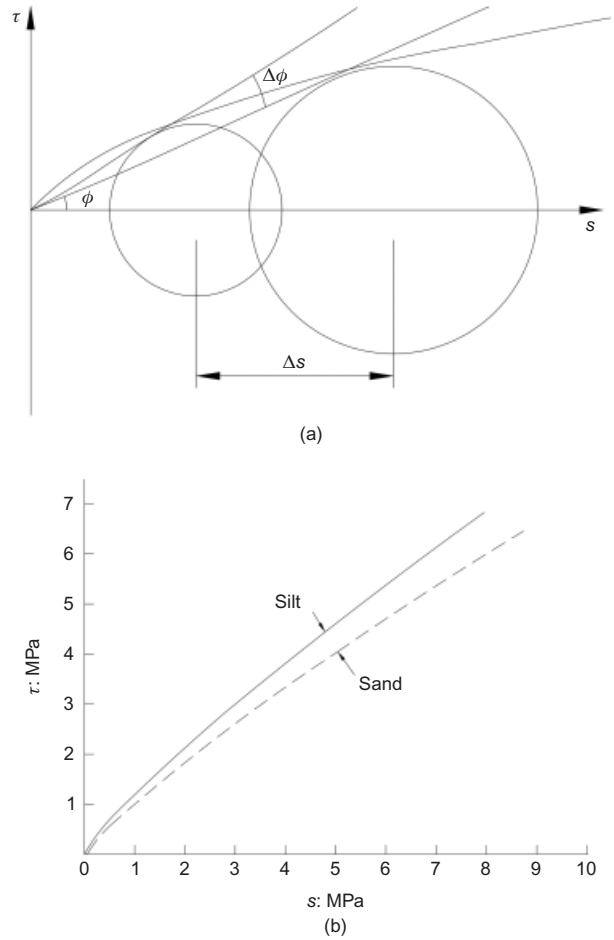

Fig. 3. (a) Typical shear strength for sands; (b) shear strength for two granular materials

of particles at the high end of the stress range, no simple straight envelope could be selected (Vesic & Clough, 1968).

EXTENDED PRANDTL EQUATION WITH VARIABLE ϕ

The Prandtl (1920) solution for a strip footing on weightless frictional soil is based on the linkage between a rotation of principal stress direction and the consequential change in principal stress magnitude. Fig. 4(a) shows a stable boundary XX between two adjacent zones, a and b. Jumping across XX would produce an infinitesimal rotation and shift of principal stresses. However, as the boundary is stable, the two zones must also share a common boundary stress (σ_x, τ_x), as shown in Fig. 4(b). By the sine rule, we have

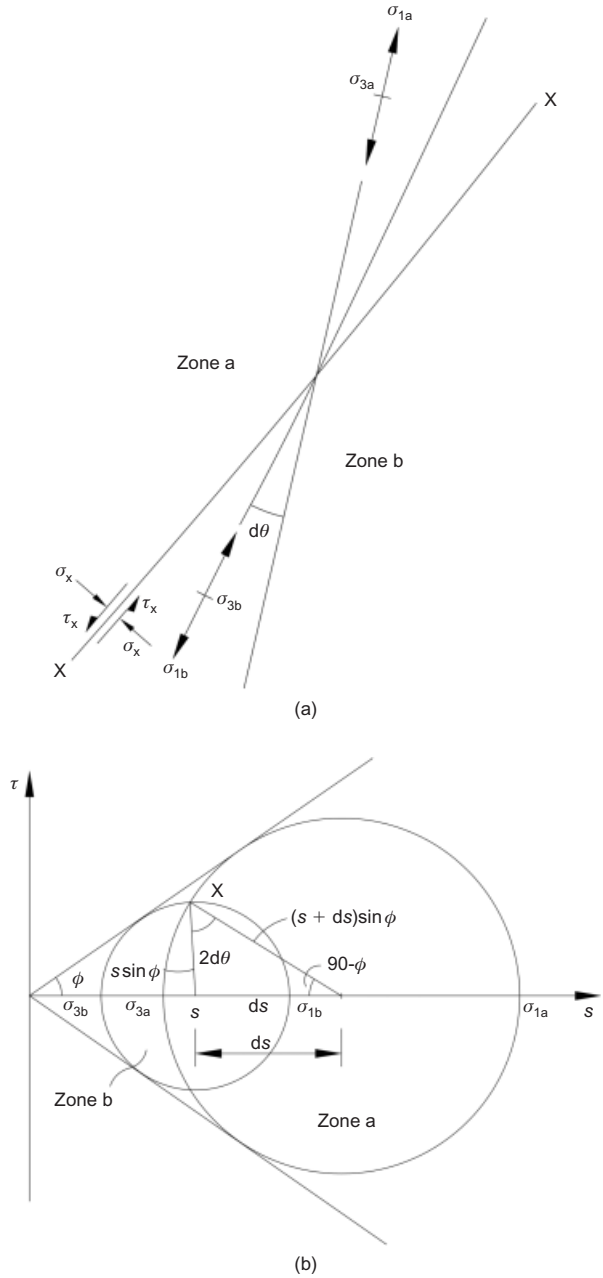

Fig. 4. (a) Neighbouring zones of limiting friction; (b) stresses in equilibrium across boundary XX

$$\frac{ds}{\sin(2d\theta)} = \frac{s\sin\phi}{\cos\phi}$$

where s is the mean stress in the plane of shear. Therefore

$$\frac{ds}{s} = 2\tan\phi d\theta \tag{1}$$

Equation (1) links the shift in the centre of a train of Mohr circles to the rotation of the direction of the major principal stress. By integrating equation (1) over the limits shown in Fig. 5, we have

$$\int_{s_o}^{s_f} \frac{ds}{s} = \int_0^{\theta} 2\tan\phi d\theta$$

$$s_f = s_o e^{2\theta\tan\phi}$$

$$\frac{\sigma_f}{1+\sin\phi} = \frac{\sigma_o}{1-\sin\phi} e^{2\theta\tan\phi}$$

Therefore

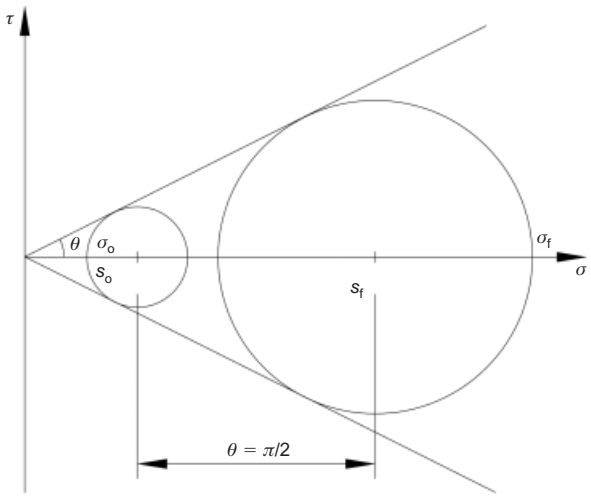

Fig. 5. Mohr circles of stress beneath a collapsing strip footing

$$\frac{\sigma_f}{\sigma_o} = \left(\frac{1+\sin\phi}{1-\sin\phi}\right) e^{2\theta\tan\phi} \tag{2}$$

For constant ϕ, and with $\theta = \pi/2$, equation (2) becomes the Prandtl equation for bearing capacity factor N_q. The discontinuities can be viewed as stress characteristics (see Fig. 6(a)). For example, travelling along characteristic D_1D_1' is equivalent to jumping across a series of the other family of characteristics, that is, D_2D_2', and vice versa. If ϕ is a function of s, this additional effect should be included in the general stress-rotation equation. Fig. 6(b) shows the geometry of a discontinuity between limiting states (s, ϕ) and (s + ds, ϕ + dϕ), where dϕ/ds has been taken positive merely for mathematical consistency. By the cosine rule we have

$$\begin{aligned} ds^2 =& s^2\sin^2\phi + (s+ds)^2(\phi+d\phi) \\ & - 2s\sin\phi(s+ds)\sin(\phi+d\phi)\cos 2d\phi \end{aligned}$$

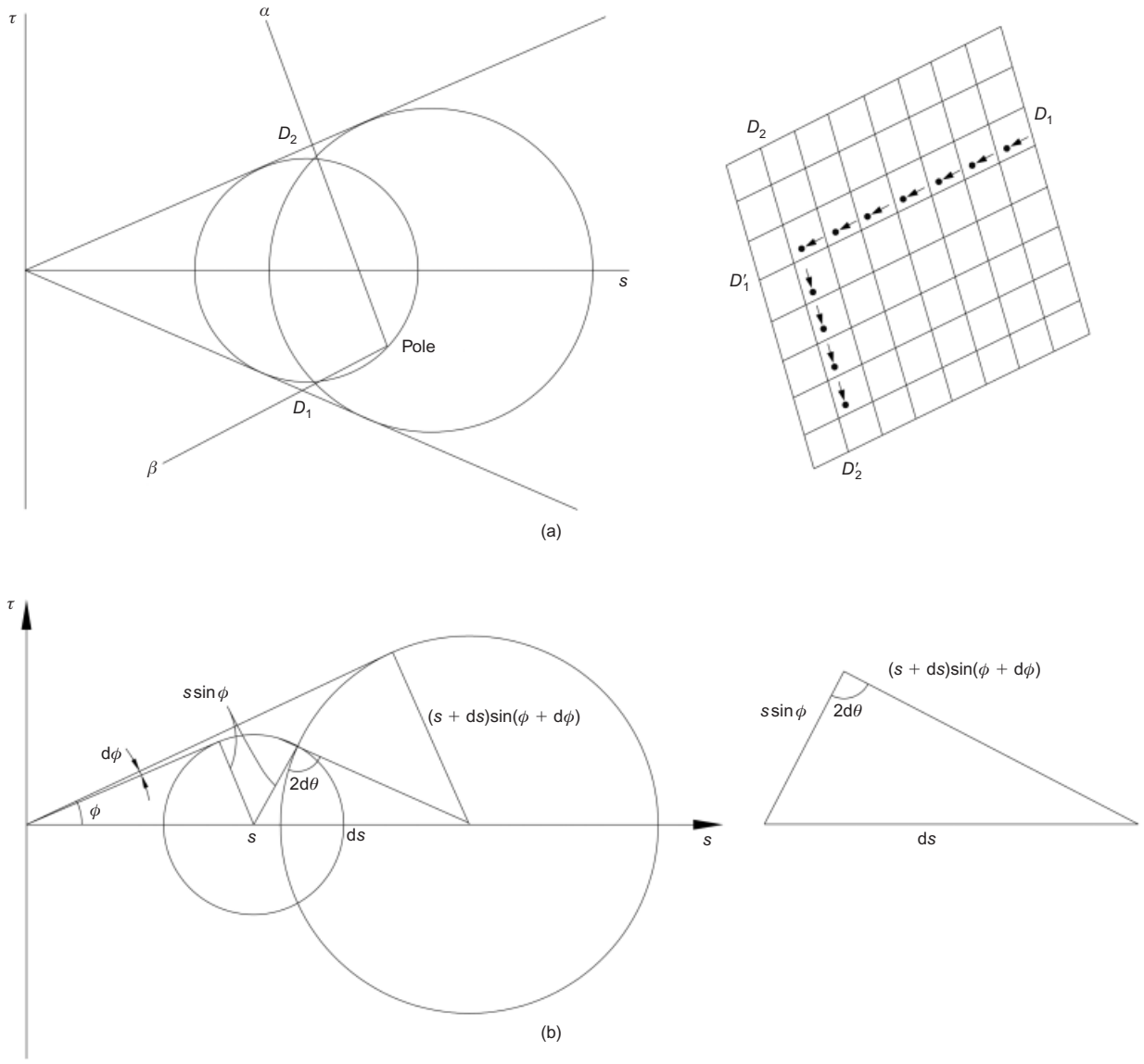

Fig. 6. (a) Mohr circles of stress across two families of discontinuities; (b) effects of varying ϕ on the stress-rotation equation

$$\left(\frac{\mathrm{d}s}{s}\right)^2 - 2\left(\frac{\mathrm{d}s}{s}\right)\tan\phi\mathrm{d}\phi - \left(4\tan^2\phi\mathrm{d}\theta^2 + \mathrm{d}\phi^2\right) = 0$$

$$\frac{\mathrm{d}s}{s} = \tan\phi\mathrm{d}\phi \pm \sqrt{\sec^2\phi\mathrm{d}\phi^2 + 4\tan^2\phi\mathrm{d}\theta^2}$$

The general stress-rotation equation can now be established as

$$\mathrm{d}\theta = \sqrt{\frac{\left(\frac{\mathrm{d}s}{s} - \tan\phi\mathrm{d}\phi\right)^2 - \sec^2\phi\mathrm{d}\phi^2}{4\tan^2\phi}} \tag{3}$$

VALIDATION OF STRESS-ROTATION EQUATION

A FORTRAN 77 program, EXPRAN, was written to evaluate N_q for a frictionless strip footing on weightless soil with ϕ varying as a function of stress s. A flow chart is shown in Fig. 7 to demonstrate how the calculation is organised. The algorithm commences by calculating ϕ in the passive zone (see Fig. 8). Initially, any arbitrary value is assumed, so that the mean stress can be written as $\sigma_o/(1 - \sin\phi)$. A new ϕ value can be derived from the functional relationship with s. Iteration is carried out by using the current ϕ to calculate the next mean stress with improved accuracy. This process continues until ϕ has achieved a target accuracy.

In the fan zone, a loading step of $\mathrm{d}s = 0{\cdot}1$ s is imposed. Likewise, the current ϕ is calculated based on the current mean stress. The amount of cumulative rotation of the principal stress direction is updated at the end of each loading step by equation (3). The active zone is deemed reached, and stress ceases to increase, when the rotation of the principal stress direction is greater than or equal to $\pi/2$. Typically, the total rotation over-ran by 0–0·04°. The bearing capacity σ_f can now be established as $s_f(1 + \sin\phi_f)$ in the active zone. The bearing capacity factor $N_q = \sigma_f/\sigma_o$ can then be calculated, appropriate to the particular value of σ_o. When σ_o is increased, ϕ reduces and N_q reduces.

An analysis with purely cohesive material that has a known exact solution (Prandtl, 1920) is selected here as a benchmark to check against the proposed algorithm. The idea is that a purely cohesive material can be viewed as a special case of ϕ varying with stress (see Fig. 9)

$$\phi = \sin^{-1}\frac{c}{s} \tag{4}$$

so that the shear strength is constant under all pressure conditions. By using equation (4) in Fig. 7, the algorithm was found to yield $\sigma_f - \sigma_o = 5{\cdot}145c$, which differs from the exact solution by only 0·07%. Therefore equation (4) in combination with a stepping routine similar to Fig. 7 has been shown to be suitable for plastic solutions with varying $\sec\phi$, at least in this simple application.

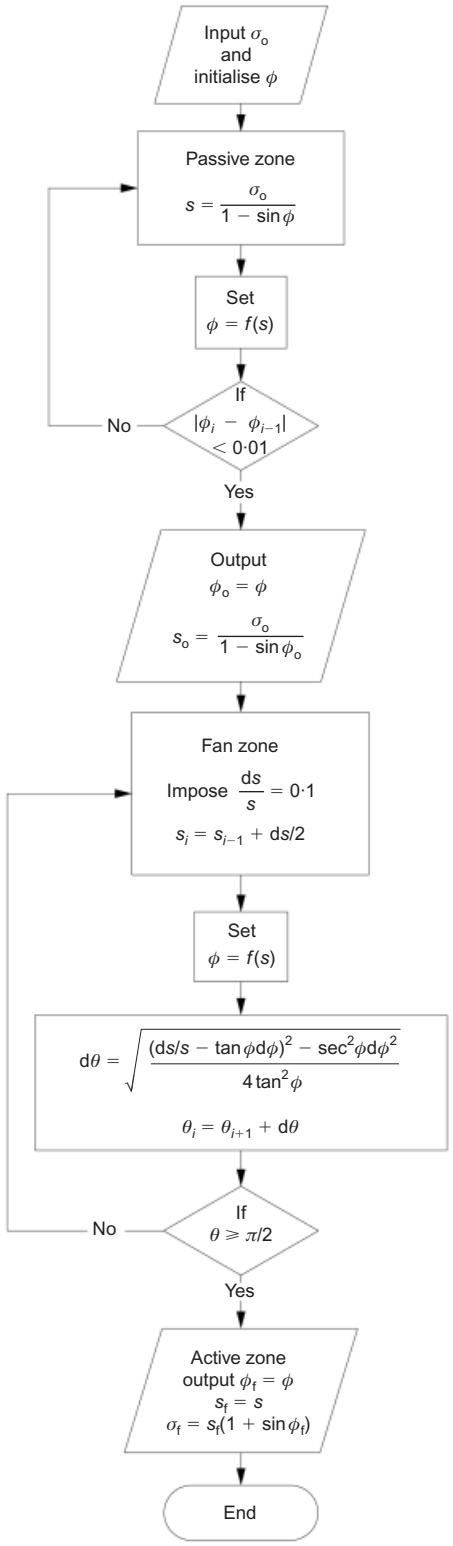

Fig. 7. Flow chart for program EXPRAN

THE METHOD OF CHARACTERISTICS WITH VARIABLE ϕ

For cases with self-weight, analytical solutions do not exist, and the method of characteristics has to be adopted. Graham & Pollock (1972), Graham & Hovan (1986) and Zhu *et al.* (2001) have incorporated ϕ as a stress-level dependent variable in their analysis by the method of characteristics. Although, during computation, ϕ is updated according to the mean stress level, they have used the same governing equations as formulated by Sokolovski (1960), in which ϕ is treated as a constant. As pointed out by Hill (1950), when ϕ is a function of mean stress, a general set of governing equations that treats ϕ as an additional variable should be formulated instead. Ueno *et al.* (2001) have treated ϕ as an additional variable, but their method is confined to plane-strain strip footings only. Alternatively, geometrical reasoning can be used to establish the effects of varying ϕ on the constant-ϕ governing equations.

In order to extend the constant-ϕ analysis so that variable-ϕ cases can also be included, the geometrical reasoning approach will be adopted. There are two effects on the governing equations when ϕ varies: the first is on the stress-

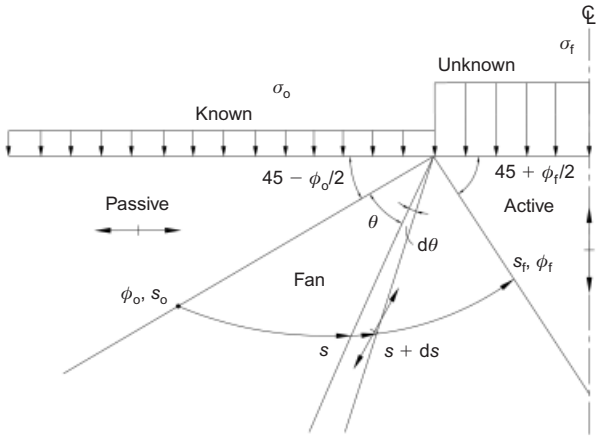

Fig. 8. Solution scheme for program EXPRAN

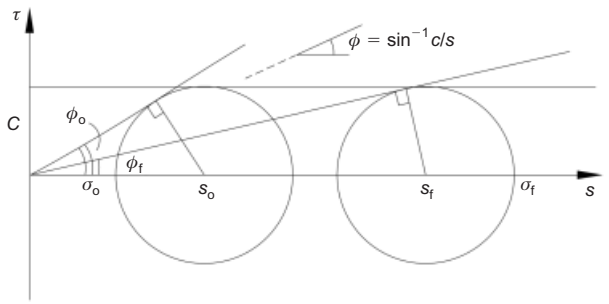

Fig. 9. Cohesion expressed in terms of sec ϕ

rotation equation, and the second is on the geometry of the characteristic lines. Both effects have to be quantified before computation can begin.

Before using the analysis to generate general predictions, it is prudent to check the method against known exact solutions. Two cases for purely cohesive material can be checked, the first for plane strain (Prandtl, 1920), and the second for axisymmetric conditions (Shield, 1955). As before, the purely cohesive soil will be treated in a variable-ϕ analysis with $\phi = \sin^{-1} c/s$. On differentiating, we obtain

$$\mathrm{d}\phi = -\frac{c\,\mathrm{d}s}{s^2 \cos\phi} \tag{5}$$

Inserting equations (4) and (5) in equation (3), we obtain

$$\frac{\mathrm{d}s}{s} = \pm 2 \sin\phi \mathrm{d}\theta$$

Comparing this with equation (1), we can define an operational constant equivalent ϕ value, ϕ_{op}, such that

$$\tan\phi_{\mathrm{op}} = \sin\phi$$

or

$$\phi_{\mathrm{op}} = \tan^{-1}(\sin\phi) \tag{6}$$

A general form of the equation can easily be derived in the same way and written as

$$\tan\phi_{op} = \frac{\tan\phi}{\sqrt{\left(1 - \tan\phi\dfrac{\mathrm{d}\phi}{\mathrm{d}\ln s}\right)^2 - \sec^2\phi\left(\dfrac{\mathrm{d}\phi}{\mathrm{d}\ln s}\right)^2}} \tag{7}$$

While equation (6) or (7) describes the value of secant ϕ and ϕ_{op} to be used in a stress-rotation equation, it does not deal with the geometry of the characteristic lines themselves. This geometry is related to the tangency of a Mohr circle on the limiting Mohr envelope. A second parameter, ϕ_{en}, must be defined as the instantaneous angle of the tangent to the strength envelope, as shown in Fig. 10.

$$\sin\phi_{\mathrm{en}} = \frac{(s + \mathrm{d}s)\sin(\phi + \mathrm{d}\phi) - s\sin\phi}{\mathrm{d}s}$$

$$= \sin\phi + s\frac{\mathrm{d}\phi}{\mathrm{d}s}\cos\phi$$

Therefore

$$\phi_{en} = \sin^{-1}\left(\sin\phi + s\frac{\mathrm{d}\phi}{\mathrm{d}s}\cos\phi\right) \tag{8}$$

Substituting equation (5) in equation (8), we have

$$\phi_{\mathrm{en}} = \sin^{-1}\left(\sin\phi - \frac{c}{s}\right)$$

$$= \sin^{-1}(\sin\phi - \sin\phi)$$

$$= 0$$

Although this was obvious for the current 'cohesion' validation, equation (8) will be used in predicting the effect of more general variation of ϕ with s.

ϕ AGAINST s: DATA FOR TYPICAL SANDS

Bolton (1986) shows that

$$\phi = \phi_{\mathrm{crit}} + \Delta I_{\mathrm{R}} \tag{9}$$

fits the data of many quartz sands, where ϕ_{crit} is treated as the constant angle mobilised in continuous shearing at constant density, and Δ is found to be 3° in triaxial tests and 5° in plane strain. The dimensionless dilatancy index I_{R} can be written as

$$I_{\mathrm{R}} = I_{\mathrm{D}} \ln\frac{p_{\mathrm{c}}}{p} - 1 \tag{10}$$

where I_{D} is the initial relative density, p_{c} is an intrinsic parameter related to the crushing of soil grains, and $p = (\sigma_1 + \sigma_2 + \sigma_2)/3$ is the mean stress at failure. Putting equation (10) in equation (9) and differentiating yields

$$\frac{\mathrm{d}\phi}{\mathrm{d}p} = -\frac{\Delta I_{\mathrm{D}}}{p} = -\frac{A}{p} \tag{11}$$

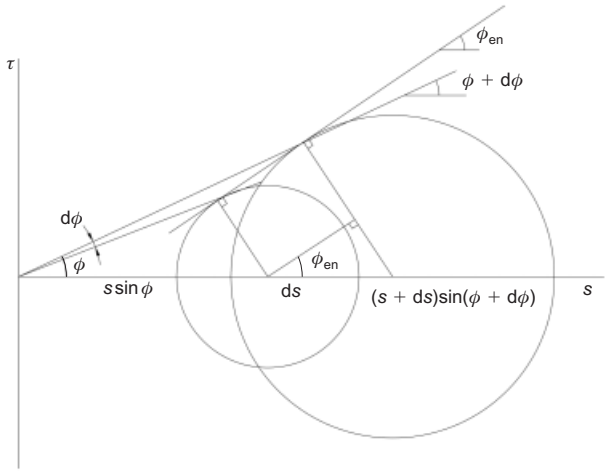

Fig. 10. Effects of varying ϕ on ϕ_{en}

where the new parameter $A = \Delta I_D$. In the work that follows no attempt has been made to discriminate between the spatial mean stress p at a point and the mean stress $s = (\sigma_1 + \sigma_3)/2$ in a plane of shearing at the same point.

Substituting equation (11) into the general stress-rotation equation (3), we have

$$d\theta^2 = \frac{ds^2}{4s^2 \tan^2 \phi}\left(1 + 2\tan\phi A - A^2\right)$$

$$\frac{ds}{s} = \frac{2\tan\phi d\theta}{\sqrt{1 + 2A\tan\phi - A^2}}$$

Comparing with the stress-rotation equation for constant ϕ

$$\frac{ds}{s} = \pm 2\tan\phi_{op} d\phi$$

as before, we can obtain

$$\tan\phi_{op} = \frac{\tan\phi}{\sqrt{1 + 2A\tan\phi - A^2}}$$

$$\phi_{op} = \tan^{-1}\left(\frac{\tan\phi}{\sqrt{1 + 2A\tan\phi - A^2}}\right) \quad (12)$$

to be used in the stress-rotation equation. Taking $A = 5I_D^\circ$ or $5I_D\pi/180$ radians, $A = 0{\cdot}087$ is obtained for the densest sands with $I_D = 1$ in plane strain, which gives $\phi_{op} \approx \phi - 2^\circ$. In all other cases the difference between ϕ_{op} and the local secant ϕ value will be smaller than 3°.

Substituting equation (11) into equation (8), we can find the envelope gradient

$$\phi_{en} = \sin^{-1}(\sin\phi - A\cos\phi) \quad (13)$$

It is easy to show that the largest deviation between ϕ and ϕ_{en} for dense soils in plane strain is about 5°. Having established ϕ_{op} and ϕ_{en}, the constant-ϕ formulation can now be extended to a realistic variable-ϕ analysis for sandy soils. The subroutine in Fig. 11 was used to calculate ϕ according to the stress level.

VALIDATION OF THE METHOD OF CHARACTERISTICS WITH VARIABLE ϕ

The method of characteristics relies on extending 'characteristic lines', which are lines of incipient shear failure, taking account of the different stress rotation and associated stress increments on two intersecting characteristics, such as QW and PW in Fig. 12. The four stress components can be expressed in terms of two dependent variables s and ψ

$$\sigma_r = s(1 - \sin\phi\cos 2\psi)$$

$$\sigma_z = s(1 + \sin\phi\cos 2\psi)$$

$$\tau_{rz} = s\sin\phi\sin 2\psi \quad (14)$$

$$\sigma_\theta = s(1 - \sin\phi) = \sigma_3$$

where ψ is the angle between the major principal stress direction and the z axis.

Along two families of stress characteristics, the governing equations become two ordinary differential equations

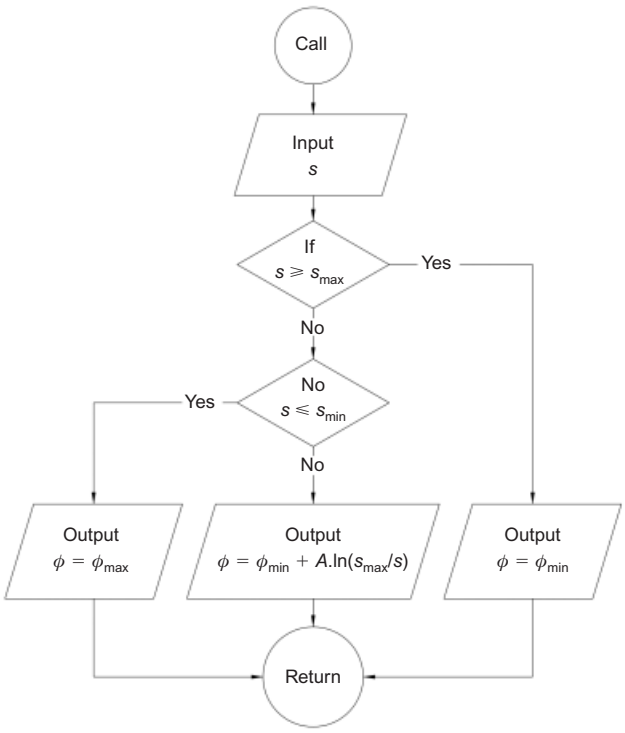

Fig. 11. Flow chart for subroutine to set ϕ

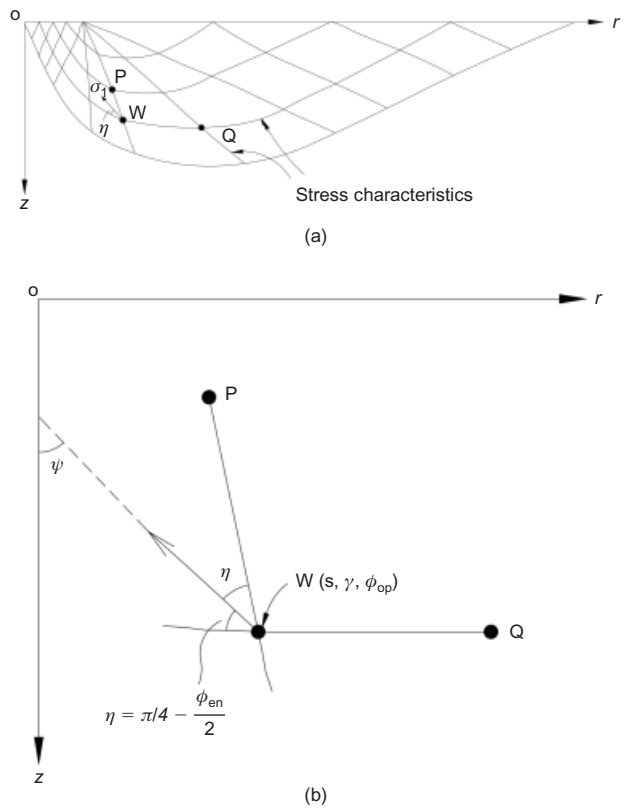

Fig. 12. (a) A typical stress characteristic mesh; (b) computation scheme of new point W from known points P and Q

$$ds\cos\phi + 2s\sin\phi d\psi + n\frac{s}{r}\left[\sin\phi\cos\phi dr + \left(\sin^2\phi - \sin\phi\right)dz\right] = \gamma(-\sin\phi dr + \cos\phi dz) \quad (15)$$

along an α characteristic given by

$$\frac{dr}{dz} = \tan(\psi - \eta)$$

and

$$ds\cos\phi - 2s\sin\phi d\psi + n\frac{s}{r}\left[\sin\phi\cos\phi dr - \left(\sin^2\phi - \sin\phi\right)dz\right] = \gamma(\sin\phi dr + \cos\phi dz) \quad (16)$$

along a β characteristic given by

$$\frac{dr}{dz} = \tan(\psi + \eta)$$

where

$$\eta = \frac{\pi}{4} - \frac{\phi}{2}$$

For the axisymmetric case we must take $n = 1$, and for the plane-strain case $n = 0$ (by inspection).

The finite-difference forms of equations (15) and (16) can be used to determine s and ψ at the point of intersection of the α and β characteristics by iteration either from a known boundary condition or from previously computed values at two adjacent points. The four stress components can then be obtained by back-substituting s and ψ into equation (14). More details about the algorithm can be obtained elsewhere (Sokolovski, 1960; Cox, 1962; Bolton & Lau, 1993). The new method additionally permits ϕ to vary from point to point, so that the geometry of the 'net' varies with ϕ_{en}, and the stress magnitude varies with ϕ_{op}.

A validation analysis for the program VARIPHI was performed for effectively weightless soil, so that it estimated bearing capacity factor N_c by performing an N_q-type analysis by the method of characteristics with varying ϕ. The plane-strain case yielded $\sigma_f - \sigma_o = 5{\cdot}14c$, which is practically the same as the exact solution, and similar to the simpler calculation procedure referred to earlier. The stress characteristics and footing pressure distribution are derived and shown in Fig. 13. It can be seen that the log spiral in the shear fan has now degenerated into a circular curve, as required.

For the axisymmetric case, the method gives $\sigma_f - \sigma_o = 5{\cdot}63c$, which differs from Shield's (1955) exact solution of $5{\cdot}69c$ by 1%. Fig. 14 compares the distribution of the calculated footing pressure distribution with Shield's solution, and shows that the present calculation gives a similar footing pressure distribution. It also shows that the characteristics are of the same shape as that calculated by Shield.

These validations have demonstrated that even with a pressure effect on $\sec\phi$ sufficient to suppress shear strength gain entirely, the method of calculation proposed here can yield a very accurate answer. It is therefore believed that this calculation procedure is suitable for application to a wide variety of soils with a general relation of ϕ against s.

PRACTICAL APPLICATIONS

In this section, prediction of the indentation pressure for a typical jack-up rig will be given as an example. Fig. 15 shows a circular footing resting on the surface of submerged dense sand with $A = 3°$, $\phi_{crit} = 37{\cdot}5°$ and $\gamma = 20$ kN/m^3, so that $\gamma' = 10$ kN/m^3.

The footing, whether dimpled, conical or flat, is assumed to be rough enough to stabilise an active zone of sand beneath the footing with a semi-angle of 28°. The inclined surface of the active cone is assumed to be acted upon by soil in which the major principal stress direction is vertical.

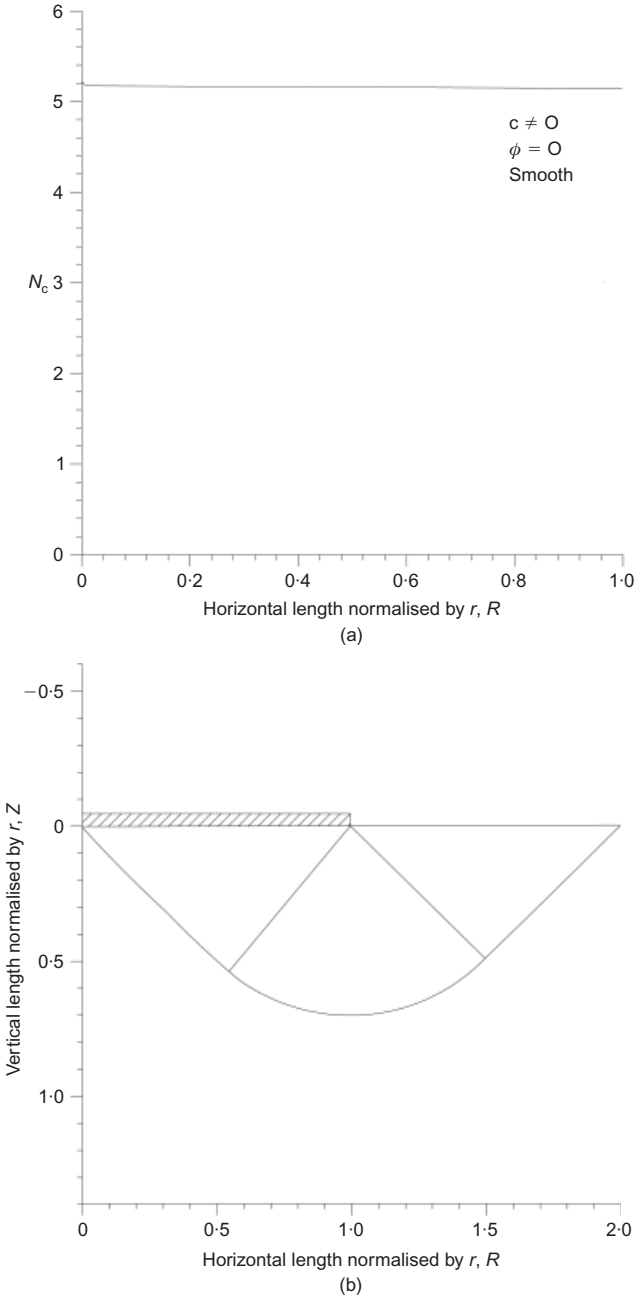

Fig. 13. Plane-strain (a) footing pressure distribution, (b) stress characteristics

This creates the boundary condition $\delta \approx \phi$ for a wide range of ϕ values in the soil near the cone. Any use of the method of characteristics demands this sort of idealisation of the relevant boundary conditions.

The results of the analysis are shown in Fig. 15, for footing diameters (at the sea bed) of 0·4 m, 1·42 m and 5·0 m. In each case, ϕ is shown to drop from its maximum value of 57° at shallow depth around the footing to much smaller values at the edge of the active cone – for example, 36° for the 5 m footing. At the same time, the bearing capacity factor N_γ has dropped by more than a factor of 3, from 712 to 207. Here N_γ is simply defined as $\sigma_f/(0{\cdot}5B\gamma')$, and σ_f is calculated as the average effective stress applied to the footing at the seabed. This calculation ignores disturbance of the sand, which would occur when a real conical footing penetrates a sand bed. It simply offers a 'snapshot' of the limiting equilibrium of a footing wished into place, permitting the size of the footing to reflect the magnitude of

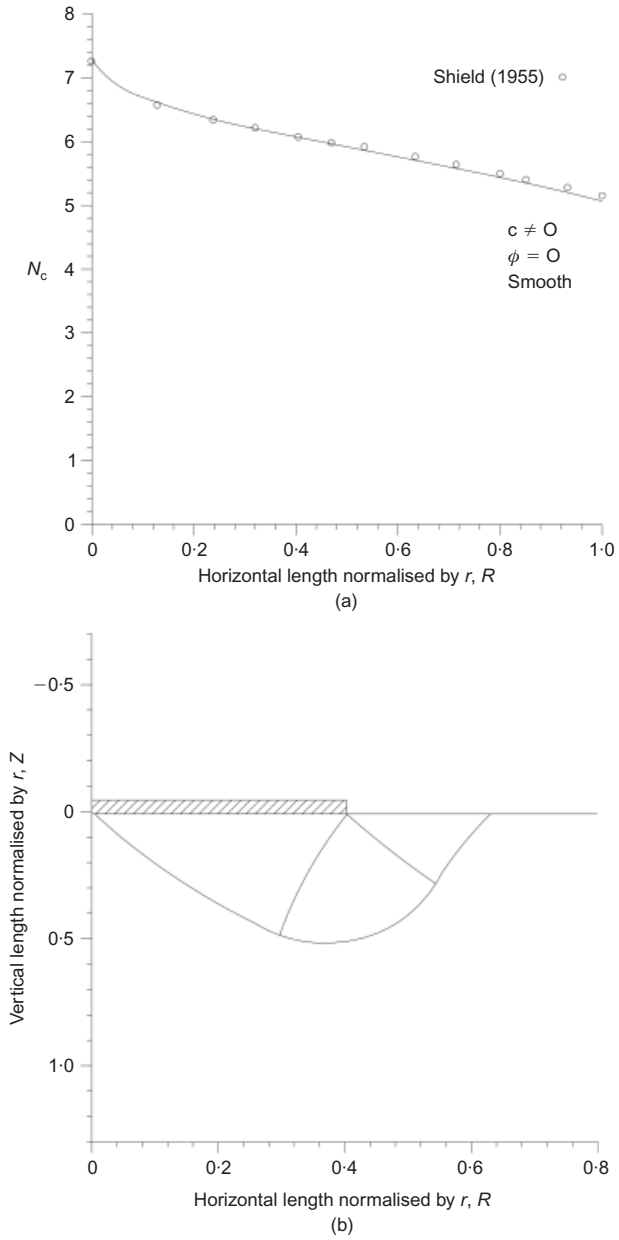

Fig. 14. Axisymmetric (a) footing pressure distribution, (b) stress characteristics

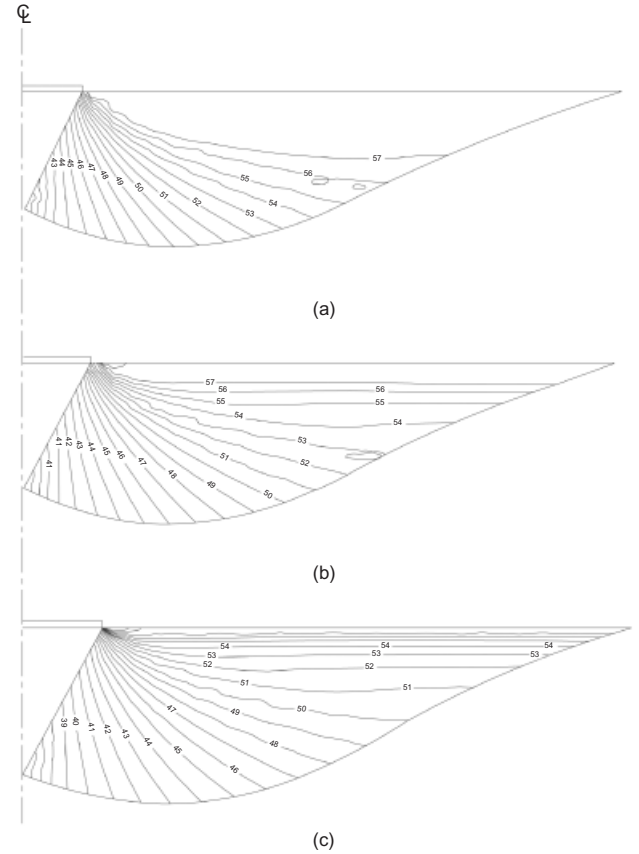

Fig. 15. Contour map of varying ϕ under rough circular footing on sand with no surcharge: (a) $B = 0{\cdot}4$ m; (b) $B = 1{\cdot}42$ m; (c) $B = 5{\cdot}0$ m

the stress, and permitting the soil to mobilise a peak angle of shearing ϕ_{max}, which is corrected for stress level using a secant variation of the type shown in Fig. 1, equivalent to the curved strength envelope shown in Fig. 3(b).

Effects such as disturbance, or progressive failure, would result in the mobilisation of $\phi_{crit} < \phi_{failure} < \phi_{max}$. Engineers must rely on experimental evidence to guide them on whether allowance must additionally be made for loss of peak strength. Our companion paper (Lau & Bolton, 2011) demonstrates that no such allowance is necessary for centrifuge models of flat footings loaded vertically to failure on sand or silt beds.

The program VARIPHI is capable of being applied directly to any problem of the limiting plastic equilibrium of granular soils, if the geometry and boundary conditions are well defined, and the variation of ϕ and s has been determined. However, a method has been found to generalise the outcome of a VARIPHI analysis for a class of problem, leaving the engineer able to use existing conventional constant-ϕ analyses with a selected mean-mobilisable angle of shearing resistance ϕ_m.

Taking the previous example of a 5 m footing on the surface of dense submerged sand, the N_γ value of 207 would, in a typical constant-ϕ analysis (Bolton & Lau, 1993), imply an equivalent constant value $\phi_m = 39{\cdot}3°$. When this is compared with the contours of ϕ_{max} shown in Fig. 15, it seems too close to the lower limit. It must be remembered, however, that variable-ϕ analysis not only influences the mean mobilised strength; it also alters the geometry of the characteristic net. The apparently low constant equivalent value $\phi_m = 39{\cdot}3°$ is that value which, when inserted in a constant-ϕ with a constant-ϕ geometry, recovers the same value of bearing capacity as a variable-ϕ analysis. ϕ_m is of some practical assistance, since it enables us to identify the equivalent mean effective stress p_m at which a triaxial test would record ϕ_m.

A number of trial calculations were performed for two different soils at a relative density of 1, namely

(*a*) sand : silica, $\phi_{max=}$ 57·5° at $s = 10$ kPa, $A = 3°$
(*b*) silt : silica, $\phi_{max=}$ 57·5° at $s = 50$ kPa, $A = 3°$

supporting circular footings at the point of plastic indentation. Two calculations were made, one on the basis of weightless soil subject to an effective overburden pressure σ_o (see Table 1), and the other for soil with self-weight and negligible surcharge (see Table 2). In the latter case, a small surcharge (with an embedment depth of much less than 1% of the footing width) was required to stabilise the surface film, but a check was made to ensure that this magnitude did not influence the bearing capacity. The nominal surcharge was needed for a purely frictional material to avoid

Table 1. Summary of results from the variable-ϕ analysis for a circular footing on weightless soil

σ_o	σ_f: kPa		$\phi_{average:}$ degrees		p_m: kPa	
	Sand	Silt	Sand	Silt	Sand	Silt
5	3 149	6 619	47·6	50·7	270	480
10	4 584	9 778	46·1	49·5	450	700
25	7 645	15 673	44·2	47·6	850	1 400
50	11 370	22 735	42·7	46·1	1 400	2 200
100	17 110	33 430	41·2	44·6	2 300	3 700
200	25 980	49 680	39·6	43·1	3 900	6 000

Table 2. Summary of results from the variable-ϕ analysis for a shallow circular footing

B: m	σ_f: kPa		$\phi_{average}$: degrees		p_m: kPa	
	Sand	Silt	Sand	Silt	Sand	Silt
0·40	1 423	3 155	44·5	47·4	760	1 500
0·90	2 161	4 670	43·0	45·9	1 250	2 400
1·42	2 735	5 943	42·1	45·1	1 700	3 100
3·00	4 017	8 720	40·5	43·7	2 900	5 000
5·00	5 165	11 410	39·3	42·8	4 200	6 900
10·00	7 435	16 180	37·8	41·3	7 200	11 000

numerical problems due to local yielding of the soil near the surface film.

The two soils were of different degrees of particle strength, the silt being five times stronger, as represented by its mobilising $\phi_{max} = 57{\cdot}5°$ at $s = 50$ kPa, whereas the sand could mobilise 57·5° at a reduced value $s = 10$ kPa. The typical rate of loss of strength $A = 3°$ invoked per unit increase in the natural logarithm of stress (from equations (9), (10) and (11)) implies that ϕ_{max} at $s = 50$ kPa for the sand would be $(57{\cdot}5° - 3\ln 5) = 52{\cdot}7°$. The companion paper (Lau & Bolton, 2011) shows these propositions fit the triaxial data of two soils fitting these descriptions. Either the silt particles may be described as five times stronger, or the silt particles as an aggregate can be described as displaying 5° more shearing resistance than the sand. Each soil loses 7° of ϕ per factor 10 increase in mean stress.

In Tables 1 and 2 the bearing capacities calculated using VARIPHI have been back-analysed to give the equivalent-constant value ϕ_m, and this in turn has been processed to find the value of mean stress p_m at which ϕ_m would have been measured in a triaxial test. In Figs 16(a) and 17(a) the values of bearing capacity coefficient (N_q or N_γ) are plotted against the relevant resisting stress (σ_o or $0{\cdot}5B\gamma'$), each on logarithmic axes (base 10), and appropriate values of ϕ_m are inserted at intervals on the bearing capacity axis. It can be seen that these two identically dense granular materials may have bearing capacity factors between about 100 and 1000, depending on the stress magnitudes. The less crushable silt has a bearing capacity about twice that of the sand, but for each soil a tenfold increase in resistive stress (σ_o or $0{\cdot}5B\gamma'$) produces roughly a threefold reduction in bearing capacity factor. In Figs 16(b) and 17(b) the values of p_m associated with ϕ_m are plotted against the harmonic mean of the resisting stress and the bearing capacity σ_f.

It will be seen that the VARIPHI calculations for the two soils can be fitted reasonably well by parabolas, in each of the figures. A reasonable approximation for both soils appears to be

$$p_m = 2\sqrt{\sigma_f \sigma_o} \quad \text{for } N_q \tag{17}$$

$$p_m = 13\sqrt{\sigma_f 0{\cdot}5B\gamma} \quad \text{for } N_\gamma \tag{18}$$

If this value of p_m is used to find ϕ_m in triaxial tests, the resulting value can be inserted into a constant-ϕ analysis to derive an appropriate bearing capacity.

CONCLUSIONS

(*a*) The stress-rotation equations used for constant-ϕ analysis need to be modified when ϕ is a function of mean stress p. These modifications have been derived and executed in a computer program that solves for equilibrium using the method of characteristics in the region of a known boundary stress condition.

(*b*) Dilative granular materials generally exhibit a linear rate of reduction of $\sec\phi$ with an increase in $\log p$. Further evidence will also be provided to support this contention in the companion paper (Lau & Bolton, 201X). In problems of plastic indentation, it has been shown that the variation in ϕ beneath a footing has a significant effect on the bearing capacity factor. Bearing capacity factors for dense sand and silt have been derived. The silt, which developed the same peak friction angle as the sand when it was subjected to five times greater confining pressure, produced bearing capacity factors approximately twice as large as the bearing capacity factors in sand. For each soil, a tenfold increase in resistive effective stress (σ_o or $0{\cdot}5B\gamma'$) caused a threefold reduction in bearing capacity factor. Looser soils, which are closer to the critical state, must be expected to be less sensitive to stress-level effects.

(*c*) If precise failure loads and plastic mechanisms are required, the new program VARIPHI must be employed. However, if only the failure loads need be estimated, an approximate treatment has been validated. The failure

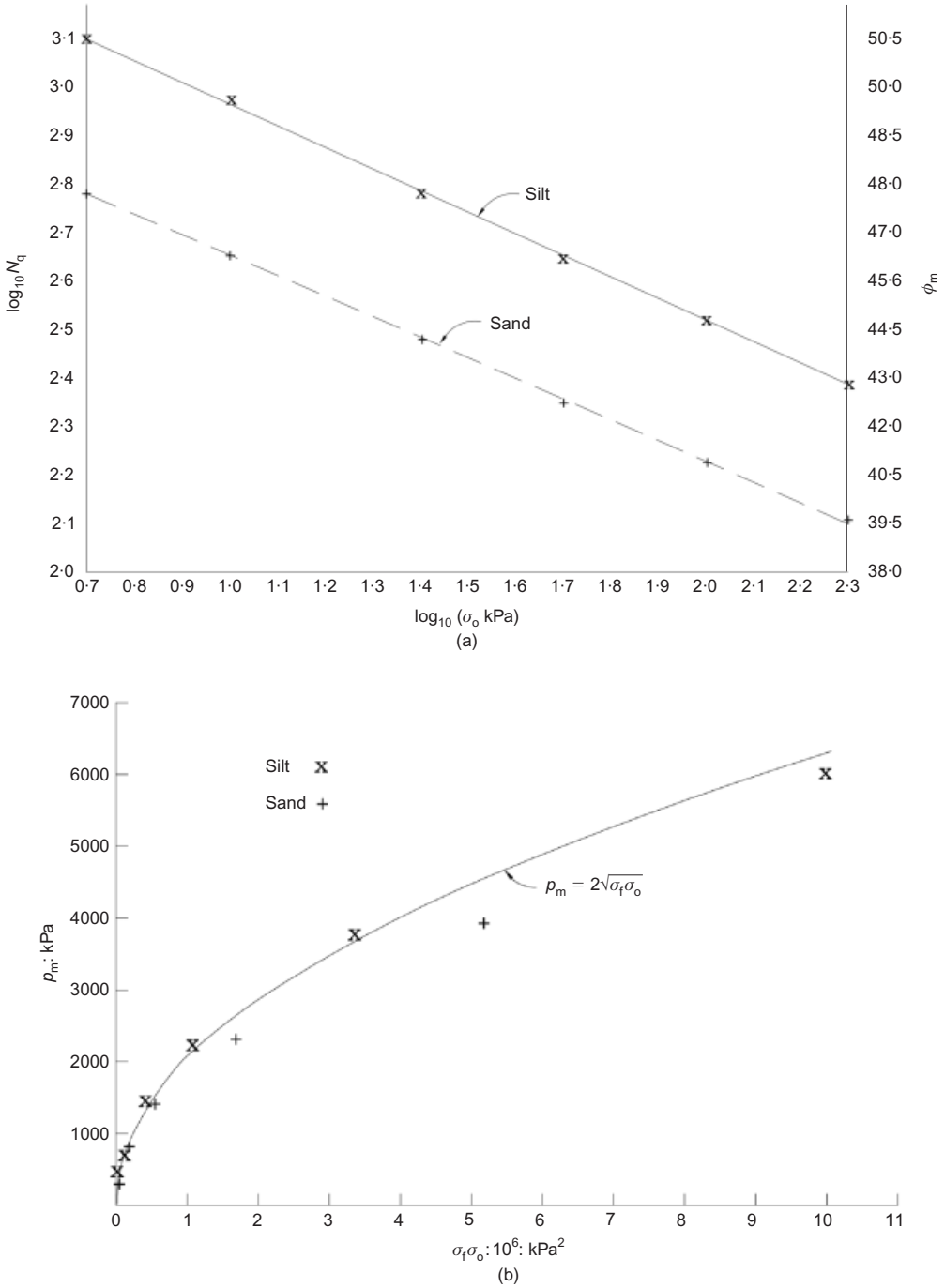

Fig. 16. (a) $\log_{10}$-$\log_{10}$ plot of N_q and σ_o; (b) empirical rule to find the average working stress in the weightless soil supporting a circular surface footing

load with VARIPHI can be equated to that running an equivalent-constant angle of shearing ϕ_m. The triaxial data of ϕ against p can be used to find the value of p_m at which $\phi = \phi_m$. Each class of problem will tend to display some functional linkage between p_m and the other imposed stresses. Two different functions have been suggested linking p_m to the harmonic mean vertical stress ($\sqrt{\sigma_f \sigma_o}$ or $\sqrt{\sigma_f 0{\cdot}5B\gamma'}$) in N_q or N_γ bearing problems.

ACKNOWLEDGEMENT

The first author is grateful for the financial support provided by the Hong Kong Croucher Foundation.

NOTATION

All stresses are effective stresses unless otherwise stated.

- A stress-induced strength reduction constant for sand
- B footing diameter
- c cohesion
- I_D relative density
- I_R relative dilatancy index
- N_c bearing capacity factor (cohesion) ($= \sigma_f/c$)
- N_q bearing capacity factor (surcharge) ($= \sigma_f/\sigma_o$)
- N_γ bearing capacity factor (self-weight) ($= \sigma_f/0{\cdot}5B\gamma$)
- p mean stress ($= (\sigma_1 + \sigma_2 + \sigma_3)/3 \approx (\sigma_1 + \sigma_3)/2$)
- p_c preconsolidation pressure
- p_m equivalent mean working stress
- R normalised radius
- r radius
- s mean stress in the plane of shear
- s_f mean stress in the active zone

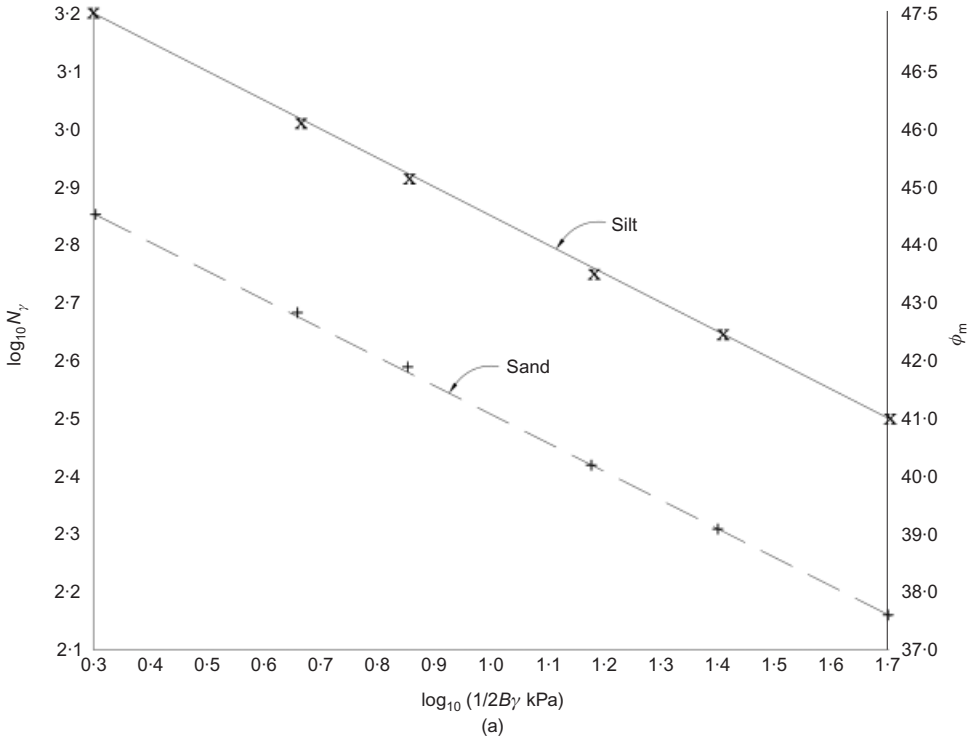

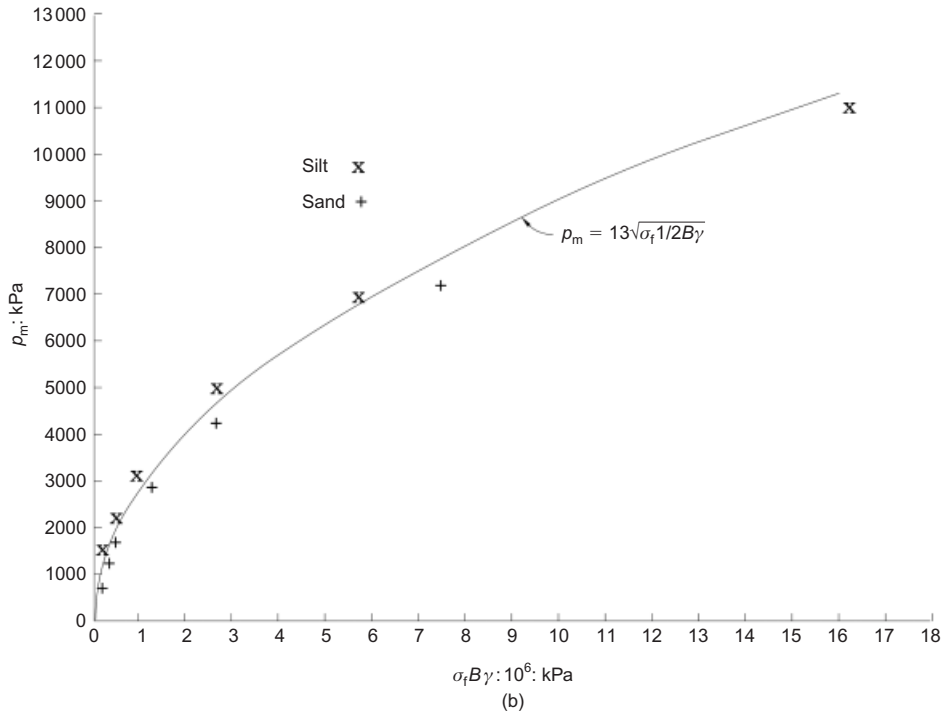

Fig. 17. (a) $\log_{10}$-$\log_{10}$ plot of N_γ and $\frac{1}{2}B\gamma$; (b) empirical rule to find the average working stress in the weightless soil supporting a circular surface footing

s_o mean stress in the passive zone
Z normalised length
α, β pair of stress characteristics
γ bulk density of soil
γ' submerged density of soil
δ cone–soil interface friction
θ principal stress rotation
σ stress
σ_1, σ_2, σ_2 principal stresses
σ_f bearing capacity
σ_o surcharge
τ shear stress
ϕ secant angle of friction
ϕ_{crit} critical state angle
ϕ_{en} angle of local strength envelope describing the stress characteristics
ϕ_m mobilised angle of friction
ϕ_{max} maximum angle of friction
ϕ_{op} operative angle of friction
ψ orientation of principal stress direction

REFERENCES

Bolton, M. D. (1986). The strength and dilatancy of sands. *Géotechnique* **36**, No. 1, 65–78, **doi**: 10.1680/geot.1986.36.1.65.

Bolton, M. D. & Lau, C. K. (1993). Vertical bearing capacity factors for circular and strip footings on Mohr Coulomb soil. *Can. Geotech. J.* **30**, No. 6, 1024–1033.

Cox, A. D. (1962). Axially-symmetric plastic deformation in soils – II. Indentation of ponderable soils. *Int. J. Mech. Sci*. **4**, No. 5, 371–380.

De Beer, E. E. (1965). Influence of the mean normal stress on the shearing strength of sand. *Proc. 6th Int. Conf. Soil Mech. Found. Engng, Montreal* 1, 165–169.

Graham, J. & Hovan, J.-M. (1986). Stress characteristics for bearing capacity in sand using a critical state model. *Can. Geotech. J.* **23**, No. 2, 195–202.

Graham, J. & Pollock, D. J. (1972). Scale dependent plasticity analysis for sand. *Civ. Engng Public Works Rev.* **67**, No. 788, 245–251.

Hill, R. (1950). *The mathematical theory of plasticity.* Oxford: Clarendon Press.

Kumar, J. & Khatri, V. N. (2008). Effect of footing width on bearing capacity factor N_γ for smooth strip footings. *J. Geotech. Geoenviron. Engng* **134**, No. 9, 1299–1310.

Kutter, B. L., Abghari, A. & Cheney, J. A. (1988). Strength parameters for bearing capacity of sand. *J. Geotech. Engng ASCE* **114**, No. 4, 491–498.

Lau, C. K. & Bolton, M. D. (2011). The bearing capacity of footings on granular soils. II: Experimental evidence. *Géotechnique*, **doi**: 10.1680/geot.7.00207.

Prandtl, L. (1920). Über die harte plastischer korper (On the hardness of plastic bodies). *Nachr. kgl. Ges. Wiss. Gottingen (Math.-phys. Klasse)*, 74–85.

Shield, R. T. (1955). On the plastic flow of metals under conditions of axial symmetry. *Proc. R. Soc. London Ser. A* **233**, No. 1193, 267–287.

Sokolovski, V. V. (1960). *Statics of soil media*. London: Butterworth (translated into English from 1942 Russian edition).

Ueno, K., Miura, K. & Maeda, Y. (1998). Prediction of ultimate bearing capacity of surface footing with regard to size effects. *Soils Found*. **38**, No. 3, 165–178.

Ueno, K., Miura, K., Kusakabe, O. & Nishimura, M. (2001). Reappraisal of size effect of bearing capacity from plastic solution. *J. Geotech. Geoenviron. Engng* **127**, No. 3, 275–281.

Vesic, A. S. & Clough, G. W. (1968). Behaviour of granular materials under high stresses. *J. Soil Mech. Found. Div. ASCE* **94**, No. SM3, 661–688.

Zhu, F., Clark, J. I. & Phillips, R. (2001). Scale effect of strip and circular footings resting on dense sand. *J. Geotech. Geoenviron. Engng* **127**, No. 7, 613–621.